Bifurcations in Morris-Lecar neuron model

Kunichika Tsumoto[†], Tetsuya Yoshinaga[‡], Kazuyuki Aihara[§] and Hiroshi Kawakami[¶]

[†] *Takuma National College of Technology, Takuma 769-1192 Japan*
tsumoto@dt.takuma-ct.ac.jp
[‡] *The University of Tokushima, Tokushima 770-8509 Japan*
yosinaga@medsci.tokushima-u.ac.jp
[§] *The University of Tokyo, Bunkyo-ku 113-8656 Japan; and*
CREST, Japan Science and Technology Co.(JST), Kawaguchi 332-0012 Japan
aihara@sat.t.u-tokyo.ac.jp
[¶] *The University of Tokushima, Tokushima 770-8506 Japan*
kawakami@ee.tokushima-u.ac.jp

Abstract

We investigate bifurcations observed in a Morris-Lecar neuron model. Especially, we paid attention to the change of bifurcation structures between type I and type II models. We found that the transition of properties between type I and II is controlled by only one-dimensional variation of a potential in a voltage-dependent function.

1. Introduction

We investigate bifurcations in a model equation of Morris-Lecar (M-L) neuron[1]. The neuronal model exhibits properties of both type I and type II membranes excitability by setting of its system parameters. It is known that neuronal models are classified by the dynamical structure that underlies the onset of autonomous periodic firing[2]. From a bifurcational point of view, the generation of the periodic firing in the type I model results from a saddle-node (tangent) bifurcation of equilibrium points. On the other hand, if the periodic firing occurs by a sub-critical Hopf bifurcation, the neuron is called a type II[4]. For example, the Hodgkin-Huxley(H-H) neuron model[3] is a typical type II model.

The M-L type I model is considered as an important model for studying dynamics in a single neuron, because pyramidal cells in the real brain have been thought to be type I neuron. Although there are lots of papers on bifurcation phenomena in the H-H neuron model, relatively little has been investigated for the M-L model[4, 5].

In Ref.[4], Rinzel and Ermentrout studied mechanisms of bifurcation using the M-L neuron model when $I_{\rm ext}$, representing the externally applied constant DC current, changes. They showed some system parameters to determine whether the property of the neuron model is type I or type II. These system parameters are the maximal conductance of Ca^{2+} current, the maximum rate constant for K^+ channel opening, a potential in a voltage-dependent function (N_∞) and the reciprocal of slope of N_∞. However, there are no discussion on bifurcation phenomena with respect to the change of properties of the neuron by varying these parameters. We are interested in how the alternation of the property of the M-L neuron is influenced by varying multiple-parameter.

In this study, we change above mentioned parameters of the M-L model over wide ranges, including those studied by Ref.[4], and consider a global structure of bifurcation in the multiple-parameter space. In particular, we pay attention to the change of bifurcation structures between type I and type II models. To calculate various bifurcations[6], we obtain two-parameter bifurcation diagrams with $I_{\rm ext}$ as the abscissa and the other parameter as the ordinate. Using these bifurcation diagrams, we identify the parameter regions in which the M-L neuron with the type I characteristic behaves. As a result, we found that the change of several parameters of the maximal conductance of Ca^{2+} current, the maximum rate constant for K^+ channel opening and the reciprocal of slope of N_∞ contributes little to alterations of the bifurcation structure. Furthermore, we clarified that a periodic solution appears through a homoclinic bifurcation.

2. M-L Neuron Model

The M-L neuron model[1] is described by

$$\begin{aligned} C_M \frac{dV}{dt} &= -g_{\rm L}(V - V_{\rm L}) - g_{\rm Ca} M_\infty (V - V_{\rm Ca}) \\ &\quad -g_{\rm K} N (V - V_{\rm K}) + I_{\rm ext} \\ \frac{dN}{dt} &= \lambda_N (N_\infty - N) \end{aligned} \tag{1}$$

where M_∞, N_∞ and λ_N, respectively, are assumed as the following functions

$$M_\infty = 0.5\,[1 + \tanh\{(V - V_1)/V_2\}] \quad (2)$$
$$N_\infty = 0.5\,[1 + \tanh\{(V - V_3)/V_4\}] \quad (3)$$
$$\lambda_N = \phi \cosh\{(V - V_3)/2V_4\} \quad (4)$$

In the following, several system parameters except for $I_{\rm ext}, g_{\rm Ca}, \phi, V_3$ and V_4, representing the applied DC current, a maximal conductance of Ca^{2+} current, a maximum rate constant for K^+ channel, a potential in the voltage-dependent function (N_∞) and the reciprocal of slope of N_∞, respectively, in Eqs.(1)–(4) are listed in Table 1.

3. Analytical Methods and Notation

Before showing results, we summarize method and notations used in bifurcation diagram. Considering a Poincaré section for a limit cycle, the analysis of limit cycles can be reduced to an analysis of fixed and periodic points of the Poincaré map. Bifurcation occurs when the topological type of a fixed point is changed by the variation of a system parameter. Bifurcations of limit cycle appeared in this paper are as follows

1. Tangent bifurcation: One of characteristic multipliers is 1. By changing a parameter, a pair of fixed or periodic points generates.

2. Homoclinic bifurcation: This global bifurcation is caused by a connection of stable and unstable manifolds of an equilibrium point. A limit cycle may generate due to the variation of system parameter.

The numerical determination of generic bifurcation values is accomplished by using the method proposed by Kawakami[6]. Moreover, for the calculation of the homoclinic bifurcation parameter and the orbit, we use the method in Refs.[7, 8].

Table 1: Fixed parameters for the M-L neuron.

C_M	=	5.0 [μF/cm^2]
$g_{\rm K}$	=	8 [μS/cm^2]
$g_{\rm l}$	=	2 [μS/cm^2]
$V_{\rm Ca}$	=	120 [mV]
$V_{\rm K}$	=	-80 [mV]
$V_{\rm l}$	=	-60 [mV]
V_1	=	-1.2 [mV]
V_2	=	18 [mV]

In the bifurcation diagram, g_ℓ and h_ℓ indicate tangent and Hopf bifurcations for equilibrium points, respectively, where ℓ indicates the number to distinguish the several same sets, if they exist. For tangent and homoclinic bifurcations of limit cycles, symbols G and H, respectively, are used.

4. Results and Discussion

By the numerical analysis, we obtained bifurcation diagrams of the $I_{\rm ext}$ versus $g_{\rm Ca}, \phi, V_3, V_4$ planes. For the limited number of pages, three bifurcation diagrams except for $I_{\rm ext}$–V_3 plane are omitted in this paper. In the following, let us consider bifurcations in the $I_{\rm ext}$–V_3 plane. Bifurcation diagram of equilibrium points and a limit cycle with $I_{\rm ext}$ as the abscissa and V_3 as the ordinate is shown in Fig. 1.

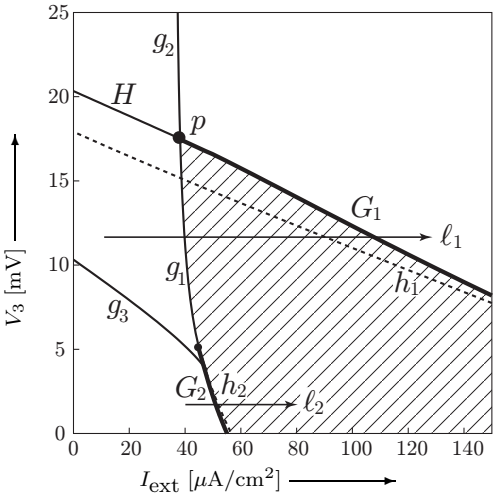

Figure 1: Bifurcation diagram for equilibrium points and a limit cycle. Fixed parameters as $g_{\rm Ca} = 4.0$ [μS/cm^2], $\phi = 1/15$ [s^{-1}], $V_4 = 17.4$ [mV]. The region ▨ indicates parameter at which a stable limit cycle exits.

First, we consider bifurcations of generation of a limit cycle. Figure 2(a) shows a one-parameter bifurcation diagram, by varying the value of $I_{\rm ext}$, for fixed value of $V_3 = 12$[mV]. By increasing the value of $I_{\rm ext}$ along the line ℓ_1 in Fig.1, the stable equilibrium point with type of ${}_0O$ causes the tangent bifurcation g_1 with saddle point with type of ${}_1O$. After this tangent bifurcation, a limit cycle generates. The phase portraits and waveforms before and after the tangent bifurcation g_1 are illustrated in Figs. 3(a)–(c). The values of $I_{\rm ext}$ labeled by (a)–(c) in Fig. 2(a) show parameters at which the attractors shown in Figs. 3(a)–(c) are observed, respectively.

Next, we show a mechanism of generation of a limit

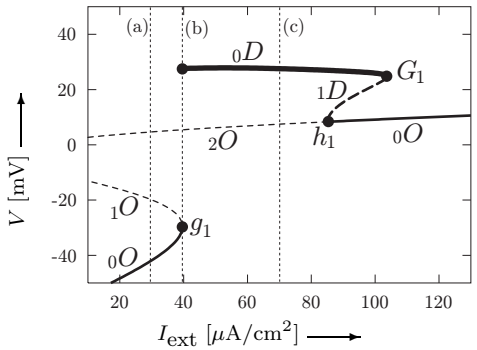

(a) $V_3 = 12$ [mV]

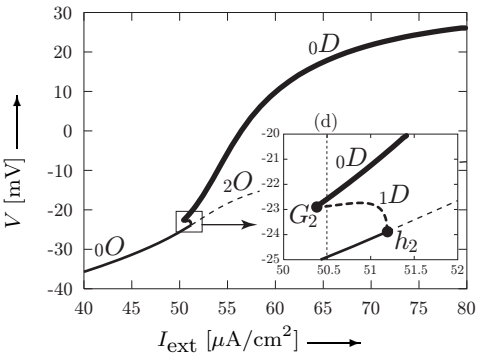

(b) $V_3 = 2$ [mV]

Figure 2: One-parameter bifurcation diagrams. In this figure, symbols with types $_0O, _1O, _2O, _0D$ and $_1D$ indicate stable, saddle, unstable equilibrium points, stable and unstable limit cycles, respectively.

cycle, when $I_{\rm ext}$ changes along the line ℓ_2 in Fig. 1. Figure 2(b) shows a one-parameter bifurcation diagram for a fixed value of $V_3 = 2$ [mV]. By increasing the value of $I_{\rm ext}$ through the Hopf bifurcation h_2, we can observe a bifurcation with formula:

$$_0O + _1D \to _2O \tag{5}$$

where the left- and right-hand sides of the arrow indicate the unstable limit cycle and equilibrium points before and after the bifurcation, respectively. The unstable limit cycle with type $_1D$ causes tangent bifurcation G_2 with stable limit cycle by decreasing the value of $I_{\rm ext}$. Figure 3(d) shows an example of trajectories. At the parameter value, stable, unstable limit cycles and stable equilibrium point coexist. We see that the stable limit cycle generates due to the tangent bifurcation with the unstable limit cycle caused via sub-critical Hopf bifurcation. Namely, when the value of V_3 is 2 [mV], the M-L neuron model exhibits as type II model.

Finally, let us consider a homoclinic bifurcation in Fig.1. By increasing the value of V_3, for a fixed value of $I_{\rm ext}$ as, e.g., 20 [μA/cm^2], a unstable limit cycle with type $_1D$ generates by Hopf bifurcation h_1. Moreover, the generated unstable limit cycle causes a homoclinic bifurcation H with formula:

$$_1O + _1D \to _1O \tag{6}$$

As a result, the unstable limit cycle disappears by the homoclinic bifurcation. In Fig. 1, the point labeled by p denotes a co-dimension three bifurcation point. Due to the co-dimension three bifurcation point, tangent bifurcations of equilibrium points are divided into two bifurcations denoted by g_1 and g_2 in Fig. 1: (1) by passing through the curve g_1, a limit cycle generates, and (2) only a stable equilibrium point remains via tangent bifurcation g_2. The first bifurcation process means that the M-L neuron exhibit as the type I model.

In the following, we discuss the alternation of the property of the M-L neuron from type I to type II. The classification of type I and II neurons was proposed by Hodgkin[2], who found arbitrarily low response frequencies and spike latencies(type I) and a narrow range of responses with no spike delay(type II). Rinzel and Ermentrout have been studied the change of properties between type I and II models from the bifurcational point of view[4, 5]. They showed system parameters to determine whether the property of the M-L neuron model is type I or type II neuron, see Table 2.

In this study, we have calculated bifurcation by changing $I_{\rm ext}$ and one of the parameters($g_{\rm Ca}, \phi, V_3$ and V_4; the parameters other than used in each bifurcation diagrams are set to the values of type I model in Table 2). The characteristic of the type I neuron is that the neuron starts periodic firing via a tangent bifurcation of equilibrium points. When $I_{\rm ext}$ is relatively small, by varying the value of V_3 from 12 [mV] to 2 [mV], the bifurcation structure changes since the tangent bifurcation with symbols of g_1 and g_3 forms cuspidul point in Fig.1. In other parameter planes, e.g., $I_{\rm ext}$–$g_{\rm Ca}$, $I_{\rm ext}$–ϕ and $I_{\rm ext}$–V_4 planes, above mentioned alternations of the bifurcation structures could not occur. As the result,

Table 2: System parameters classified as Type I and II model[4, 5].

parameter	type I	type II
$g_{\rm Ca}$ [μS/cm^2]	4.0	4.4
ϕ [s$^-$1]	1/15	1/25
V_3 [mV]	12	2
V_4 [mV]	17.4	30

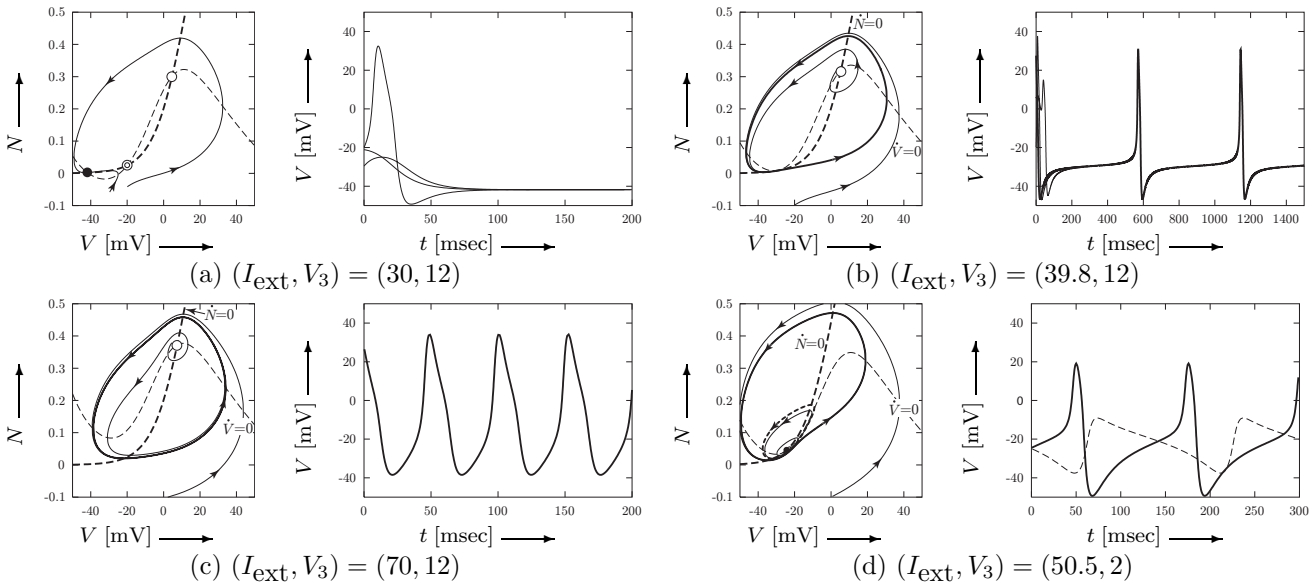

Figure 3: Examples of trajectories observed in Eq.(1). In phase portraits, the black, white and double circles denote a stable, an unstable and a saddle equilibrium points, respectively. The arrow indicates the direction of trajectory in phase portraits. The heavy solid and dashed lines of closed curve, respectively are a stable limit cycle and an unstable limit cycle. The light and heavy dashed lines indicate the V– and N–nullclines in Eq.(1), respectively.

we see that the alternation of property of the M-L neuron can be controlled by changing the only parameter V_3, representing the potential in the voltage-dependent function in Eq.(3).

5. Conclusions

We have investigated bifurcations in the M-L neuron model. The main results of the analysis are summarized as follows: (1) We have clarified that the transition of property between type I and II is controlled by only one-dimensional variation of the potential in a voltage-dependent function. (2) The change of several parameters of the maximal conductance of Ca^{2+} current, the maximum rate constant for K^+ channel opening and the reciprocal of slope of N_∞ contributes little to alterations of the bifurcation structure.

Analysis of a synaptically coupled M-L neuron with the property of type I is an interesting future problem to be considered.

References

[1] C. Morris and H. Lecar: "Voltage oscillations in the barnacle giant muscle fiber," *Biophys. J.*, vol.35, pp.193–213, 1981.

[2] A. L. Hodgkin, "The local changes associated with repetitive action in a non-modulated axon," *J. physiol. (London)*, vol.107, pp.165–181, 1948.

[3] A. L. Hodgkin and A. F. Huxley, "A qualitative description of membrane current and its application to conduction and excitation in nerve," *J. Physiol. (London)*, vol.117, pp.500–544, 1952.

[4] J. Rinzel and G. B. Ermentrout: "Analysis of neuronal excitability and oscillations," In C. Koch and I. Segev(Eds.), *Methods in Neuronal Modeling : From Synapses to Networks,* MIT press, London, 1989.

[5] B.S. Gutkin and G.B. Ermentrout: "Dynamics of membrane excitability determine interspike interval variability: A link between spike generation mechanisms and cortical spike train statistics," *Neural Comput.*, vol.10, pp.1047–1065, 1998.

[6] H. Kawakami, "Bifurcation of periodic responses in forced dynamic nonlinear circuits: computation of bifurcation values of the system parameters," *IEEE Trans. Circuits and Systems*, vol.CAS-31, no.3, pp.246–260, 1984.

[7] H. Kawakami and Y. Ozaki, 'Analysis of a separatrix loop in n-dimensional autonomous system,' IECE Trans., vol.J67-A, no.11, pp.1098–1099, 1984 (in Japanese).

[8] T. Yoshinaga and H. Kawakami, 'Bifurcation and chaotic state in forced oscillatory circuits containing saturable inductors,' In L. Pecora and T. Carroll(Eds.), *Nonlinear Dynamics in Circuits*, pp.89–119, World Scientific, 1995.